The surface density gradient of grafted poly (ethylene glycol): preparation, characterization and protein adsorption

Y.S. Lin, **V. Hlady**, and **C.-G. Gölander**[1]
The center for Biopolymers at Interfaces, Departments of Bioengineering and Materials Science and Engineering, University of Utah, Salt Lake City, UT 84112, USA

Abstract

A surface density gradient of grafted poly (ethylene glycol) (PEG) chains was prepared using two-phase silanization of a flat silica surface. The first step was to create the surface density gradient of isocyanatopropyldimethylsilyl groups and to hydrolyze the isocyanato moiety into an amine. These surface amines were reacted with an excess of aldehyde-terminated PEG. The PEG–silica surface was characterized by dynamic contact angle measurements, X-ray photoelectron spectroscopy and ellipsometry. The length of the PEG gradient region was approximately 7 mm and the thickness in air ranged from zero to 1.1 nm. The maximum surface density of the PEG layer, as calculated from ellipsometric data, amounted to an average 0.4 PEG (molecular weight M_w = 2000 Da) molecule nm^{-2}, while the surface density average of the amine groups was 1.4 molecules nm^{-2}, indicating that only a fraction of the surface amines reacted with aldehyde-terminated PEG. The PEG segment density profile in the gradient PEG region was computed by a self-consistent mean field theory. The PEG (M_w = 2000 Da) segments profile was not parabolic, but showed a thin depletion zone next to the surface.

The influence of the surface density of the grafted PEG chains on protein repellence was tested by the adsorption of fibrinogen from solution and from a ternary protein solution mixture containing fibrinogen, albumin and immunoglobulin G. Fibrinogen adsorption onto the silica end of the gradient was extremely low, both in the presence of the other two proteins and in their absence. As the surface density of the grafted PEG chains increased, so did the fibrinogen adsorption (up to 0.024 µg cm^{-2}). It is not clear whether this low fibrinogen adsorption resulted from the interactions of the protein with the grafted PEG chains or with residual surface amines that were available due to some imperfections in the grafted PEG layer.

Keywords

Grafted poly (ethylene glycol); Protein adsorption; Surface density gradient

1. Introduction

The interest in protein-repellent surfaces originates from the fact that many foreign surfaces adsorb proteins when exposed to blood or other protein-containing solutions. The surface adsorption of proteins from blood may initiate the activation of blood coagulation, or of the complement system or some other undesired processes. Similar situations, with less drastic endings, occur when a foreign surface comes into contact with protein-containing body fluids, such as tears or urine. The non-specific adsorption of proteins is a nuisance in solid phase immunoassays and in other clinical diagnostic procedures.

Poly (ethylene glycol)s (PEGs) have been widely used as colloid stabilizers in foods, paints and pharmaceutical products. Studies showed that PEG has protein-repellent and cell-repellent properties and that the PEG coatings do not elicit antigenic activity [1]. Initial work on protein-repellent PEG surfaces was followed by an increasing number of biomedical applications, such as PEG-encapsulated enzymes [2], incorporation of PEG into polyurethane-based biomaterials [3] and many others. Advances in this field have been summarized in a recent monograph [4]. A simple theory of protein–surface interactions in the presence of a tethered PEG surface layer has been proposed by Jeon and Andrade [5]. In their analysis these authors have calculated osmotic and elastic contributions to the steric repulsion free energy using a "brush" polymer layer model derived from the de Gennes "blob" concept [6]. More recent theories of tethered polymer layers use a self-consistent mean field approach. Continuum self-consistent mean field theory predicts a parabolic segment density profile of tethered polymer chains in good solvent [7–9]. The theory assumes strongly stretched grafted chains and can be solved analytically. However, because of this assumption, it can only be rigorously applied to tethered chains that are very long. In contrast, lattice models of the self-consistent mean field theory are applicable to polymers of all sizes [10–13]. Because of the complexity of the random walk in a potential field, lattice self-consistent mean field theories are usually solved numerically on a computer. No attempts have been made, to our best knowledge, to predict protein repellence using the self-consistent mean field approach.

Our interest is to understand the mechanism of PEG protein repellence. In the case of a grafted PEG layer, the distribution of the PEG segments in the layer is expected to determine the protein repellence. The PEG segment distribution depends not only on the surface density of the polymer chains but also on the interactions between the PEG segments, solvent and surface. The effect of the PEG surface density is very important: while a low surface density may not provide significant steric exclusion, a high surface density may not allow enough mobility to the grafted PEG chains. In order to study the effect of the PEG surface density on protein repellence, one typically needs to perform extensive experimental work as follows: (1) to prepare a set of surfaces, each with different surface density of the PEG chains;(2) to characterize each surface;(3) to measure protein adsorption on each surface.

Prime and Whitesides [14] have used the self-assembly of a mixture of oligomeric PEG–alkane thiols and non-PEG–alkane thiols to build a set of surface films on gold, each with a different surface density of PEG chains. Others have used the self-assembly of a mixture of

PEG-lipids and non-PEG-lipids to build protein-repellent liposomes [15]. Instead of using multiple PEG surfaces we decided to prepare a gradient PEG–silica surface. The concept of the gradient surface was originally demonstrated in 1988 by Elwing et al. [16] who prepared a hydrophilic–hydrophobic surface gradient on a silicon wafer. We have modified their procedure to prepare different types of surface gradient on flat silica [17–19]. In order to fully utilize the advantage of a single macroscopic surface with a surface gradient we have developed an internal reflection fluorescence technique and an autoradiography technique to measure the spatial distribution of adsorbed protein molecules along the gradient dimension [18,20]. One of the gradient surfaces that we used for the protein adsorption study was the amine surface density gradient [21]. The amine groups of the surface amine density gradient could be further reacted with aldehyde-terminated soluble polymer. The reaction of aldehyde-terminated PEG with the gradient of the surface amines should result in a macroscopic gradient of terminally-attached PEG chains on which the number of PEG chains decreases smoothly from a certain maximum surface density to zero along one of the linear surface dimensions. The use of a single gradient PEG silica surface circumvents a number of experimental difficulties associated with the preparation and characterization of multiple surfaces. In this paper, we describe the preparation and characterization of such gradient PEG surfaces on flat silica. The experimental results of the PEG gradient characterization are compared with the segment density profile of tethered PEG chain segments calculated with the self-consistent mean field theory of Scheutjens and Fleer [10–12]. We also test the gradient PEG–silica surface for protein-repellent properties by measuring the adsorption of fibrinogen from buffer solutions and from protein ternary mixtures.

2. Experimental

The chemistry of grafting the PEG chains to the silica surface comprised several steps:

1. preparing aldehyde-terminated PEG (CH_3O–PEG–CHO);

2. preparing fused silica with surface amine groups;

3. reacting CH_3O–PEG–CHO with surface amines;

4. reducing the formed imminium salt with cyanoborohydride anion.

Both homogeneous and gradient PEG–silica surfaces were prepared using PEG polymers with molecular weights (M_w) 2000 Da and 5000 Da respectively.

2.1. Preparation of aldehyde-terminated PEG (CH_3O–PEG–CHO)

Dimethyl sulfoxide (DMSO)–acetic anhydride oxidation was used to prepare CH_3O–PEG–CHO from CH_3O–PEG–OH: 2.5 g of poly (ethylene glycol) monomethyl ether (PEG2000; Aldrich; M_w = 2000Da) were added to 0.273 ml of acetic anhydride in 11.03 ml of DMSO and the mixture was stirred for 30 h at room temperature. At this point the reaction mixture was added dropwise to 100 ml of dry ethyl ether, followed by reprecipitation two or three times from methylene choride with ethyl ether. It was necessary to dehydrate the DMSO, CH_3O–PEG–OH and all glassware in order to obtain a high yield of aldehyde groups (around 85%). The formation of the aldehyde was periodically checked during the reaction

with use of the Schiff test. The Schiff reagent was prepared by adding 2 g of sodium bisulfite to a 200 ml solution containing 0.2 g of *p*-rosaniline hydrochloride and 2 ml of concentrated hydrochloric. The Schiff test produces a colored product with glutaraldehyde (molar extinction coefficient $\varepsilon = 657$ M^{-1} cm^{-1} at 530 nm). In the case of CH$_3$O–PEG–CHO the wavelength, λ_{max} shifted to 560 nm and an accurate extinction coefficient was not known. Nonetheless, the Schiff test provided a comparison of aldehyde yields.

2.2. Preparation of the homogeneous PEG–silica surface

The aminopropyldimethylsilyl silica surfaces (APDMS–silica) were prepared by the acidic hydrolysis of the isocyanatopropyldimethylsilyl silica surfaces (IPS–silica) [21]. Figure 1 shows the schematics of the surface reactions. The IPS–silica was prepared by immersing a clean dry fused-silica plate (2.5×7.5 cm^2; Esco) in 0.1% (v/v) isocyanatopropyldimethylchlorosilane (IPS; Petrarch Systems Inc.) solution in trichloroethylene (TCE; Merck) for 90 min. After immersion the silica plate was rinsed with TCE and was dried under an N$_2$ gas jet. The APDMS–silica was prepared from the IPS–silica by incubation in an acidic solution at pH 3.8 at 50°C for 0.5 h. The CH$_3$O–PEG–CHO was reacted with the amine groups of the APDMS–silica surface in the aqueous solution. The reaction was performed in two steps. The first step was carried out in a less-than-good solvent for PEG, 11% (w/w) K$_2$SO$_4$, in order to collapse the chains and achieve a higher polymer surface density. A 50 mg ml^{-1} solution of CH$_3$O–PEG–CHO was reacted with the APDMS surface at 60°C in acetate buffer solution (pH 5.2; 11% (w/w) K$_2$SO$_4$) for 40 h. The second step was the reduction of the Schiff base, which was achieved by adding 50 µl of NaCNBH$_3$ aqueous solution (0.42 g in 5 ml of distilled water) for each 1 ml of acetate buffer solution and reacting it for 4 h.

2.3. Preparation of the gradient PEG–silica surface

The strategy for preparing the surface density gradient of PEG chains on the silica surface was to create a gradient of amine groups on the silica in a separate reaction and then to react the CH$_3$O–PEG–CHO polymer with the surface amines. The surface density gradient of the amine groups on silica was prepared using the two-phase diffusion technique as described previously [21]. Prior to silanization, the silica plates were cleaned in chromosulfuric acid for 40 min at 70°C, rinsed thoroughly in triply distilled water, dried in an N$_2$ jet and mounted in a 200 ml glass beaker. In the beaker, 75 ml of a 0.1% (v/v) solution of IPS in denser trichloroethylene (density $d = 1.4$ g cm^{-3}), was gently injected under the 75 ml solution of lighter *p*-xylene (Fluka; $d = 0.9$ g cm^{-3}). IPS was allowed to diffuse from the lower phase into the *p*-xylene. During the diffusion, IPS reacted with the silica surface. After 1.5 h the beaker was emptied through a drainage pipe. The plates were thoroughly rinsed from above with trichloroethylene and dried in an N$_2$ gas jet. The newly created IPS gradient surface was immersed in aqueous solution (pH 3.8; 50°C) for 0.5 h to hydrolyze the surface isocyanato groups to amines. The subsequent grafting of the CH$_3$O–PEG–CHO chains was performed as described above (see Fig. 1).

2.4. Characterization of the PEG–silica surfaces

All surface modification steps were followed by X-ray photoelectron spectroscopy (XPS), the Wilhelmy plate technique and ellipsometry. The XPS analysis was performed on only non-gradient surfaces using an XPS spectrometer (Hewlett-Packard 5950B). Deconvolution of the XPS spectra was performed by means of a curve-fitting program. In particular, the CH_3O–PEG–silica surfaces were characterized by XPS binding energies and intensities of the carbon C1s spectrum [22]. The efficiency of grafting the CH_3O–PEG–CHO chains to the APDMS surface was deduced from the ratio of the XPS intensities of the ether carbon atom (originating from PEG) and alkyl carbon atom (originating from APDMS). The advancing and receding water contact angles were measured by the Wilhelmy plate technique. The modified silica plates were immersed at a speed of 10 mm min^{-1} through the air/water interface while the plate weight was continuously recorded.

The surface densities of the APDMS groups and PEG chains were determined by ellipsometry in air (Rudolf Research Model AR2000). For the ellipsometry measurements, the APDMS and the CH_3O–PEG–silica surfaces were prepared on a silicon oxide layer 125 nm thick on a silicon wafer surface (Si/SiO_2) instead of on the fused-silica plates. Control experiments were performed on the Si/SiO_2 and $Si/SiO_2/APDMS$ surfaces. The ellipsometric measurements were not accurate enough to calculate independently the refractive index n and the thickness d of each layer. Instead, an average refractive index, n_{av} = 1.44, was calculated from several ellipsometric measurements (three or more) and was then kept fixed in the calculation of the thickness of each layer. Once the thickness of each layer was determined, the composition of each surface layer was calculated using the one component Lorentz-Lorenz equation [23a]. The molar refractivity of CH_3O–PEG–CHO was calculated from the molar refractivity of the constituent atoms (C 2.591; H 1.028; O 1.643; N 2.376; Si 4.881). By assuming that PEG has the formula CH_3O–$(CH_2$–CH_2–$O)_{44}$–CH_2-, the molar refractivity was calculated to be 496.197. Similarly, the molar refractivity of APDMS was calculated to be 34.604.

Characterization of the APDMS and PEG gradient surfaces was performed with the Wilhelmy plate technique and ellipsometry. The advancing and receding water contact angles were measured as a function of the position along the gradient, i.e. along the plates' longest dimension. The thickness of the CH_3O–PEG surface layer was measured incrementally along the gradient using ellipsometry and the average refractive index n_{av} = 1.44. The spatial resolution was determined by the size of the laser beam; it was approximately 0.5 mm.

2.5. Calculation of segment density distribution of grafted PEG

The distribution of PEG segments in the CH_3O–PEG surface layer was calculated as a function of the PEG surface density with the self-consistent field theory of Scheutjens and Fleer [10–12]. The theory only counts the interactions of nearest neighbors in the system and calculates the most probable distribution of each component by minimizing the free energy of the whole system. The calculation was run on a SUN workstation using the GOLIAD program [23b]. The grafted PEG was modeled as a sequence X $[(CCO)_{45}]$ B, where 45 is equal to the number of segments in the 2000 Da polymer chain. The two end groups, the

terminal methoxy group and the covalent bond of CH_3O–PEG and the APDMS nitrogen, were represented by B and X respectively. The other components in the system were water (W) and the surface (S). The Flory–Huggins interaction parameter χ_{YZ}, defined as the energy change (in kT) associated with the transfer of a segment of type Y from a solution of pure Y to a solution of pure Z, was used to account for the energy of mixing. The interaction parameters for each pair of components in the system are listed in Table 1. The values of the parameters χ_{CO}, χ_{CW} and χ_{WO}, were taken from the work of Barneveld [23b]. The negative value of χ_{WO} indicated the affinity of water for the PEG segment oxygen. The χ_{CS} and χ_{BS} values were assumed to be 0.5. In order to ensure that the PEG chain is covalently bonded to the surface, the χ_{XS}, value was incrementally decreased until all X segments in the system were found to be in contact with the surface. The value of $-300\ kT$ was low enough to simulate an irreversible bonding of B with S. All other interaction parameters were assumed to be zero, indicating that these components have neither a specific affinity nor an aversion for each other. A flat diamond lattice (spacing assumed to be equal to one-third of a monomer unit, 0.10 nm [24]) and a temperature of 298 K were used in the calculations.

2.6. Protein adsorption

Human serum albumin (HSA; ICN ImmunoBiologicals), and human immunoglobulin G (IgG; Cappel Labs) were used as received. Human fibrinogen (Fgn; Calbiochem) was labeled with carrier-free [125]I (100 mCi ml^{-1}; Amersham) by the chloramine-T method as described by Lin et al. [25]. The efficiency of the ^{125}I labelling was determined by precipitating the labeled protein with 20% trichloroacetic acid (TCA; Sigma) in the presence of bovine serum albumin (BSA) as a carrier protein. The amount of fibrinogen-bound ^{125}I was determined by subtracting the radioactivity of the supernatant from the total radioactivity of the solution. The ^{125}I/Fgn ratio was approximately 1/300. The final concentration of the ^{125}I labeled protein solution was determined spectrophotometrically at 280 nm. The protein absorption extinction coefficients ε (ml mg^{-1} cm^{-1}) used were 0.54 (HSA), 1.35 (IgG) and 1.625 (Fgn) respectively [26].

Protein adsorption onto the gradient PEG–silica surface took place from buffered protein solutions of concentrations corresponding to 1/10 of an average physiological value (4.2 mg Alb per milliliter; 1.3 mg IgG per milliliter; 0.32 mg Fgn per milliliter respectively). Two types of experiment were performed. In the first type, the solution contained only ^{125}I labeled Fgn + Fgn and the adsorption of ^{125}I labeled fibrinogen was measured. In the second type of experiment, two other unlabeled proteins were also present; the solution contained ^{125}I labeled Fgn + Fgn + Alb + IgG so that only the adsorption of ^{125}I-labeled fibrinogen was measured while all four proteins were adsorbing at the same time onto the surface. The adsorption was carried out at room temperature in a dual-channel flow cell. Typically, 2 ml of protein solution were injected at a flow rate of approximately 1 ml min^{-1} in each flow channel, each of which was filled prior to the injection with 0.15 M phosphate-buffered saline (PBS; pH 7.4). At the end of a 12 h incubation the channels were flushed with the PBS buffer (6 ml) avoiding the formation of an air/water interface. After the buffer wash the adsorbed protein molecules were fixed by injecting 3 ml of a freshly prepared solution of 0.6% (w/v) glutaraldehyde in PBS buffer into the flow channel. Five minutes after both channels were emptied, the flow cell was taken apart, and the amount of adsorbed

proteins on the gradient PEG–silica surface was determined by autoradiography. A detailed protocol of the adsorption experiments and autoradiographic detection of the adsorbed protein can be found elsewhere [20].

3. Results

3.1. XPS analysis

Table 2 summarizes the efficiency of the CH$_3$O–PEG–CHO grafting to the APDMS surface. The –CO–/–CH$_2$– is the ratio of ether carbon atoms (originating from PEG) and alkyl carbon atoms (originating from APDMS) calculated from the respective areas of the deconvoluted XPS C1s spectrum. The reaction between CH$_3$O–PEG–CHO and APDMS–silica at higher pH values (pH 7.2 and 9.2) was not successful; practically no ether carbon atoms were detected. If the reduction of the Shiff base was omitted, the bond between CH$_3$O–PEG–CHO and the surface amine was not stable: the –CO–/–CH$_2$– ratio decreased to 1.1.

A typical XPS carbon C1s spectrum of a homogeneous PEG–silica surface (M_w = 5000 Da) is shown in Fig. 2. Deconvolution of the spectra showed two contributions with respective binding energies of 286 eV and 284 eV. The 284 eV contribution originated from alkyl APDMS carbon atoms and the 286 eV contribution was from the ether carbon atom of PEG. The dominating 286 eV contribution indicated a successful binding reaction between CH$_3$O–PEG–CHO and APDMS–silica.

The binding energies and the relative areas of the N1s doublet peak of the APDMS–silica surface before and after the reaction with CH$_3$O–PEG–CHO are listed in Table 3. The lower energy XPS peak of the N1s doublet is often interpreted as originating from free amines and the higher energy XPS peak is thought to be due to protonated and hydrogen-bonded amines [27]. According to Moses et al. [28], the amine groups on the silica surface exist in three forms: (1) free amines which resist protonation in acid and contribute only to the lower energy XPS peak; (2) a form that resists deprotonation and contributes only to the higher energy XPS peak; (3) an active, reversibly protonated form that will contribute to both peaks depending on the acidity of the environment. The presence of the active amines on APDMS–silica can be deduced from the 10% change in the higher and lower binding energy peak areas after the exposure of the APDMS–silica to acidic conditions (Table 3). After the reaction with CH$_3$O–PEG–CHO the higher energy N1s contribution decreases by another 7%, indicating that only a fraction of the surface amines can be used for further chemical reactions. Table 4 summarizes the atomic composition of the homogeneous PEG—silica surfaces.

3.2. Wetting of APDMS– and PEG–silica gradient surfaces

Figure 3(a) shows advancing, θ_{adv}, and receding, θ_{rec}, water contact angles for the APDMS–silica gradient surface measured at two different pH values. The APDMS end of the gradient surface at pH 3.1 displayed values of 52° for θ_{adv} and 23° for θ_{rec}. The contact angles gradually decreased to zero in the gradient transition region. The hysteresis of the contact angles on the APDMS end of the gradient surface (θ_{adv}– θ_{rec} = 29°) was possibly due to the heterogeneous distribution of APDMS groups on the silica [21]. At pH 7.1 the contact

angles increased to 56° (θ_{adv})and 32° (θ_{rec}) on the APDMS end of the gradient surface. These larger contact angles can be expected to be due to deprotonation of the amine groups in the environment of higher pH: the pK_a value for the amine groups on the silica surface is 3.9 [29]. The dynamic water contact angles for the gradient PEG–silica surface at pH 7.1 are shown in Fig. 3(b): the PEG end of the surface density PEG gradient displayed contact angles of 34° (θ_{adv})and 24° (θ_{rec}). These angles did not change with pH.

3.3. Ellipsometry

The ellipsometry of a homogeneous APDMS surface showed that the APDMS layer had an average thickness of 0.3 ± 0.02 nm in air. The average thickness of the homogeneous CH_3O–PEG layer in air was a further 1.25 ± 0.31 nm. The standard deviation was determined from the measurement of eight samples. In the ellipsometric calculation of the layer thickness the average refractive index of the APDMS and PEG films was used and kept fixed at $n_{av} = 1.44$.

The surface density of the APDMS and PEG molecules in each layer was calculated separately using the ellipsometric thickness of a given layer and the molar refractivity of the molecule. The one-component Lorentz–Lorenz equation was used [23a]. The average surface density of APDMS and PEG ($M_w = 2000$ Da) were 1.4 molecules nm^{-2} and 0.4 molecule nm^{-2} respectively. The ellipsometry indicated that on average there will be seven APDMS residues and two CH_3O–PEG chains on an area of 5 nm^2. The excess of APDMS residues was in general agreement with the surface amine reactivity deduced from the XPS N1s analysis (Table 3). The variation of the average ratio APDMS/CH_3O–PEG was as high as $\pm 30\%$.

The combined ellipsometric thickness of CH_3O–PEG + APDMS layers of PEG gradient on the Si/SiO2 substrate is shown as a function of the distance along the gradient dimension in Fig. 4. The maximal thickness was 1.1 nm, which was somewhat smaller than in the case of homogeneous PEG–silica and gradually decreased to zero in the gradient transition region. The length of the transition zone was approximately 7 mm, comparable to the length determined by the dynamic water contact angle measurements (Fig. 3(b)).

3.4. Segment density profile in the grafted PEG layer

The results of the self-consistent mean field calculation of the segment density profile in the PEG grafted layers are summarized in Fig. 5. The volume fraction of the CCO segments in the layers next to the solid/water interface is shown in Fig. 5(a) as a function of the surface density of PEG. The latter parameter is expressed in terms of equivalent monolayers, Θ. Based on ellipsometry and geometric considerations, the maximal Θ value for the PEG–silica surface ($M_w = 2000$ Da) is around 1.8: the range of Θ values from 0 to 1.8 is thus approximately equivalent to the PEG surface density of the experimentally prepared gradient surface.

The density profile of the CCO segments was not parabolic for any Θ value. Rather, it showed a very thin depletion zone next to the surface: the volume fraction in the first CCO layer was less than 0.005. There were practically no CCO segments in the layers numbered

30 and above (i.e. at distances greater than 3 nm). At $\Theta = 0.1$, the CCO segments extended into the solution for up to 15 layers (or 1.5 nm), albeit with a very small volume fraction (less than 0.01).

The volume fractions of the terminal B (CH_3–) group is shown in Fig. 5(b). One recalls that the interaction parameters of this end group were chosen to be the same as for the C (–CH_2–) group in the hypothetical PEG chain. However, the overall distribution of the terminal group did not resemble the distribution of the CCO segment: the hypothetical methoxy group had a broader distribution than the CCO segment and, on average, was positioned further away from the surface. At $\Theta = 1.8$ the highest volume fraction of this end group was located at layer number 14 (or 1.4 nm away from the surface).

3.5. Protein adsorption

Figures 6(a)–6(d) show the adsorbed amounts of fibrinogen as a function of the distance along the gradient PEG–silica surface. The adsorption of fibrinogen from the ternary protein mixture was very low across the gradient PEG–silica surfaces (adsorbed amount $\Gamma < 0.003$ μg cm^{-2}, Figs. 6(a) and 6(b)). Fibrinogen adsorption from the single protein solution onto the silica end of the gradient surface was also very low ($\Gamma < 0.003$ μg cm^{-2}). At the surface density of the grafted PEG chains increased, so did the fibrinogen adsorption: somewhat higher adsorption was measured on the PEG end of the gradient PEG5000 surface ($\Gamma = 0.024$ μg cm^{-2}, Fig. 6(d)) than on the PEG2000 surface ($\Gamma = 0.009$ μg cm^{-2}, Fig. 6(c)).

4. Discussion

The objective of this study was to prepare a surface density gradient of grafted PEG chains on a silica surface for protein adsorption studies. The strategy for this was to create a gradient of reactive amine groups on the silica as a first step and then to react the surface amines with aldehyde-terminated PEG. The amine surface gradient was prepared by a silanization reaction in two layered organic solvents. The monofunctional reagent isocyanatopropyl-dimethylchlorosilane (IPS) was used as the silanization reagent. Acid hydrolysis of IPS–silica resulted in the APDMS–silica surface. The pH dependence of the water contact angles of the APDMS–silica indicated that some surface amines could be reversibly protonated at acidic conditions. The average surface density of the APDMS groups derived from ellipsometry was 1.4 groups nm^{-2} which translates to approximately half monolayer coverage based on the geometric packing argument. Accordingly, in the gradient region the average amine surface density changed from 1.4 groups nm^{-2} to zero. This relatively low surface coverage of surface amines was appropriate for further reaction with CH_3O–PEG–CHO owing to the larger size of the PEG molecules.

The grafting of CH_3O–PEG–CHO to the APDMS surface at pH 7.2 and 9.2 was not successful; the carbon atom of the aldehyde group undergoes a nucleophilic attack by a nitrogen atom more) readily at pH 5.2 than at higher pH values. The pK_a value of the surface amine groups is lower ($pK_a = 3.9$) than the pK_a of the solution amines [29]. Thus the nitrogen atom is deprotonated at pH 5.2 and nucleophilic attack on the carbon atom readily occurs. The reduction of the formed Shiff base was necessary to ensure a stable bond between PEG and a surface amine. Without it, the reaction resulted in a low PEG surface

coverage, as indicated by the ether/alkyl carbon atom ratio (Table 2). The lower binding energy component of the N1s doublet peak of the APDMS silica surface after reaction with CH_3O–PEG– CHO was centered at 399.3 eV, indicating a mixture of –CH–N–CH_2– or – CH–N=CH– bonds. Apparently, reduction of the formed –CH–N=CH– bonds by $NaCNBH_3$ may not be complete.

The water contact angle values for the PEG surfaces reported in the literature range from 50° (static contact angle; the –CO–/–CH_2– ratio equals 0.8 [30]) to 70° for the advancing and 35° for the receding contact angles respectively [31]. These published contact angles possibly indicate an incomplete coverage of PEG chains so that the underlying substrate "showed through" in the contact angles. In the present study the advancing and receding contact angles for the PEG end of the gradient surface were 34° and 24° respectively. Furthermore, the contact angles for the gradient PEG–silica surface were not influenced by the change of pH. The low contact angle values, together with the relatively high –CO–/– CH_2– ratios (Table 2), indicated that the PEG coverage on the PEG end of the gradient surface was high enough to screen the influence of residual amine groups.

The ellipsometry indicated that the ratio APDMS/CH_3O–PEG is not equal to 1: on average only two out of the seven APDMS residues on an area of 5 nm^2 were bound to PEG molecules; the other five remained unreacted. These results were also corroborated by the XPS N1s analysis. The maximal surface density of the PEG chains ($M_w = 2000$ Da) at the PEG end of the gradient surface was approximately 1.8 equivalent PEG monolayers. The limiting factor for achieving a higher PEG surface density was probably steric exclusion between the PEG chains during the surface grafting reaction, rather than too low a density of surface amines. The grafted PEG coils were overlapping with each other: the Flory radius for a PEG coil in a good solvent is 2.8 nm and the average distance between the PEG chains at the maximal coverage is 1.8 nm (based on an average of 0.4 PEG molecule nm^{-2}). The lengths of the APDMS and PEG surface gradients, as determined by the contact angle and ellipsometric measurements, were quite similar, indicating that Si/SiO_2 surface reactions were very similar to those of fused silica. It is not known whether the average ratio of APDMS/CH_3O–PEG remains constant along the gradient so that a certain fraction of the surface amines is inactive regardless of the total amine surface density. Horner et al. [32] found that some protonated amines are situated closer to the silica surface and may form hydrogen bonds with the surface silanol groups.

The self-consistent mean field simulation of the segment density profile in the hypothetical PEG grafted layers showed a non-parabolic profile of PEG segments and a very thin PEG segment depletion zone close to the surface. In addition, the hypothetical methoxy group had a broader distribution than the PEG segments and, on average, was positioned further away from the surface. A surface with such a segment density profile is expected to repel proteins. A protein colliding with the PEG layer would be able to compress the PEG segments in the outer region of the polymer layer due to a very low PEG volume fraction. However, further compression would result in a free energy penalty due to the osmotic contributions of the repulsive steric exclusion force. If the compression continued even further, an elastic restoring force would develop due to a significant loss of configurational entropy [13]. We have measured the local steric repulsion forces between an atomic force microscope probe

and the PEG layer of the PEG–APDMS–silica surface and found that they agree with the predictions of the self-consistent mean field theory [33]. The fibrinogen adsorption results are, therefore, somewhat surprising because the fibrinogen adsorption increases with the PEG surface density. It should be noted that this increase amounted to very low adsorbed amounts, between 0.009 and 0.024 μg cm^{-2}, which is much less than those reported in the literature. For example, Gombotz et al. reported that 0.35 μg cm^{-2} of fibrinogen adsorbed from a 0.2 mg ml^{-1} fibrinogen solution onto a quartz surface with grafted PEG (M_w = 2000 Da) [30], and van Damme reported that 0.15 μg cm^{-2} of fibrinogen adsorbed onto a glass surface with grafted PEG (M_w = 400 Da) [31].

Prime and Whitesides [14] suggested that weak protein adsorption onto an ethylene-oxide oligomer grafted surface may occur and may not be detected experimentally. In this study the separation of free from adsorbed fibrinogen was made by a gentle wash step. After this separation step a glutaraldehyde was used to cross-link the protein before the air/solid interface swept the adsorbed areas. In addition, we have employed a very sensitive autoradiographic technique to detect fibrinogen adsorption. It is possible that the small amounts of adsorbed fibrinogen detected on the PEG gradient surfaces may originate from a certain degree of non-homogeneity of the PEG layer or perhaps from interactions with the residual amine propyl chains. The problem of heterogeneity of surface grafted layers is not unique to gradient surfaces. However, one disadvantage of using the gradient surfaces is that microscopic characterization of the gradient region is difficult. Were the PEG molecules distributed randomly in the PEG gradient or not? Only indirect evidence is presently available to answer this question. The colloidal gold decoration of quaternary amine gradient surfaces prepared by the same IPS–to–APDMS conversion method proved that the surface amines are distributed in a patch-like form at higher surface density of amines [21]. A similar conclusion was derived from a fluorescence study of pyrenylpropyl-dimethylchlorosilyl (PPS) silica [34]. However, the patch-like distribution of amines does not necessarily have to translate into distinct polymer patches: the larger size of the polymer chains is expected to smooth out to some degree the uneven distribution of surface amines at higher surface coverage.

Contrary to some results from the literature, the silica end of the PEG gradient surface showed very low adsorption of fibrinogen. For example, Elwing et al. [35] measured 0.24 μg cm^{-2} of human Fgn adsorbed on hydrophilic silica (θ = 40°) after a 1 h incubation with 1 mg ml^{-1} of Fgn in PBS. Nygren and Stenberg [36] measured only 0.034 μg cm^{-2} human Fgn adsorbed on hydrophilic silica (contact angle θ = 28°) after a 20 h incubation with 0.187 mg ml^{-1} Fgn in PBS, ionic strength, 0.01 M. Neither of these two hydrophilic silicas were fully wettable. The tentative conclusion that less Fgn adsorbs on a fully hydrophilic surface [37,38] is indeed supported by this study.

Fibrinogen adsorption from a ternary protein mixture showed even smaller adsorbed amounts, presumably due to the blocking of the potential adsorption sites by the other two smaller proteins. Further studies are warranted to resolve the role of protein size in PEG protein repellence.

5. Conclusions

A surface density gradient of grafted PEG chains was prepared using two-phase silanization of a flat silica surface. The first step was to create a surface density gradient of isocyanatopropyldimethylsilyl groups and to hydrolyze the isocyanato part to an amine. The surface amines were further reacted with an excess of aldehyde-terminated PEG. The PEG–silica surface was characterized by dynamic contact angle measurements, XPS spectroscopy and ellipsometry. The highest surface density of the PEG layer, as calculated from ellipsometric data, amounted to an average of 0.4 PEG ($M_w = 2000$ Da) molecules nm^{-2}, while the average surface density of the amine groups was 1.4 molecules nm^{-2}, indicating that only a fraction of the amines reacted with aldehyde-terminated PEG. The length of the PEG gradient region was approximately 7 mm and the average polymer layer thickness ranged from 0 to 1.1 nm. The PEG segment density profile in the gradient PEG region was computed by a self-consistent mean field theory. The PEG ($M_w = 2000$ Da) segments profile was not parabolic, but showed a thin depletion zone next to the surface.

The influence of the surface density of the grafted PEG chains on the protein repellence was tested by the adsorption of fibrinogen from solution and from a ternary protein mixture containing fibrinogen, albumin and immunoglobulin G. The fibrinogen adsorption onto the silica end of the gradient was extremely low, both in the presence of the other two proteins and in their absence. As the surface density of the grafted PEG chains increased, so did the fibrinogen adsorption (up to 0.024 μg cm^{-2}). Although this adsorbed amount is much lower than that reported in the literature for similar PEG systems, it is not clear whether the adsorption resulted from the interactions between the PEG chains and fibrinogen, or from the interactions between protein and the underlying residual amines and imperfections in the grafted PEG layer.

Acknowledgments

References

1. Nakao A, Nagaoka S, Mori Y. J Biomat Appl. 1987; 2:219.
2. Abuchowski A, van Es T, Palczuk NC, Davis FF. J Biol Chem. 1977; 252:3578. [PubMed: 405385]
3. Sa da Costa V, Brier-Russell D, Trudel G III, Waugh DF, Salzman EW, Merrill EW. J Colloid Interface Sci. 1980; 76:594.
4. Harris, JM., editor. Poly(ethylene glycol) Chemistry; Biotechnical and Biomedical Applications. Plenum; New York: 1992.
5. Jeon SL, Andrade JD. J Colloid Interface Sci. 1991; 142:159.
6. de Gennes PG. Ann Chem. 1987; 77:389.
7. Zhulina EB, Borisov OV, Priamitsyn VA. J Colloid Interface Sci. 1990; 137:495.
8. Milner ST, Witten TA, Cates ME. Macromolecules. 1988; 21:2610.
9. Milner ST. Europhys Lett. 1988; 7:695.
10. Scheutjens JMHM, Fleer GJ. J Phys Chem. 1979; 83:1619.
11. Scheutjens JMHM, Fleer GJ. J Phys Chem. 1980; 84:178.

12. van Lent B, Scheutjens JMHM. Macromolecules. 1989; 22:1931.

13. Björling M. Macromolecules. 1992; 25:3956.

14. Prime KL, Whitesides GM. J Am Chem Soc. 1993; 115:10714.

15. Woodle MC, Lasic DD. Biochim Biophys Acta. 1992; 1113:171. [PubMed: 1510996]

16. Elwing H, Nilsson B, Svensson K-E, Askendahl A, Nilsson UR, Lundström I. J Colloid Interface Sci. 1988; 125:139.

17. Gölander C-G, Lin Y-S, Hlady V, Andrade JD. Colloids Surfaces. 1990; 49:289.

18. Hlady V. Appl Spectrosc. 1991; 45:246.

19. Lin VHlady Y-S. Colloids Surfaces B: Biointerfaces. 1994; 2:481–491.

20. Lin Y-S, Hlady J, Janatova V. Biomaterials. 1992; 13:497. [PubMed: 1321678]

21. Lin Y-S, Hlady V. Colloids Surfaces B: Biointerfaces. in press.

22. Kiss E, Gölander C-G, Eriksson JC. Prog Colloid Polym Sci. 1987; 74:113.

23a. Cupers PA, Corsel JW, Janssen MP, Kop JMM, Hermens WTh, Hemker HC. J Biol Chem. 1983; 258:2426. [PubMed: 6822569]

23b. Barneveld, PA. PhD Thesis. Wageningen University; 1991.

24. Ben Ouada H, Hommel H, Legrand AP, Balard H, Papirer E. J Colloid Interface Sci. 1988; 122:441.

25. Lin J-N, Andrade JD, Chang I-N. J Immunol Methods. 1989; 125:67. [PubMed: 2558139]

26. Haeberli, A., editor. Human Protein Data. VCH; Weinheim: 1992.

27. Vandenberg ET, Bertilsson L, Liedberg B, Uvdal K, Erlandsson R, Elwing H, Lundström I. J Colloid Interface Sci. 1991; 147:103.

28. Moses PR, Wier LM, Lennox JC, Finklea HO, Lenhard JR, Murray RW. Anal Chem. 1978; 50:576.

29. Leyden, DE.; Dill, JA. Silanes, Surfaces and Interfaces. Leyden, DE., editor. Vol. 1. Gordon and Breach Science; New York: 1986. p. 545

30. Gombotz WR, Guanghui W, Horbett TA, Hoffman AS. J Biomed Mater Res. 1991; 25:1547. [PubMed: 1839026]

31. van Damme, H. Ph D Thesis. University of Twente; 1990.

32. Horner MR, Boerio FJ, Clearfield HM. J Adhes Sci Technol. 1992; 6:1.

33. Lea AS, Andrade JD, Hlady V. Colloids Surfaces A: Physicochemical and Engineering Aspects. in press.

34. Lochmüller CH, Colborn AS, Hunnicutt ML, Harris JM. Anal Chem. 1983; 55:1344.

35. Elwing H, Askendal A, Lundström I. J Biomed Mater Res. 1987; 21:1023. [PubMed: 3654686]

36. Nygren H, Stenberg M. J Biomed Mater Res. 1988; 22:1. [PubMed: 2830287]

37. Morrissey BW. Ann NY Acad Sci. 1977; 283:50.
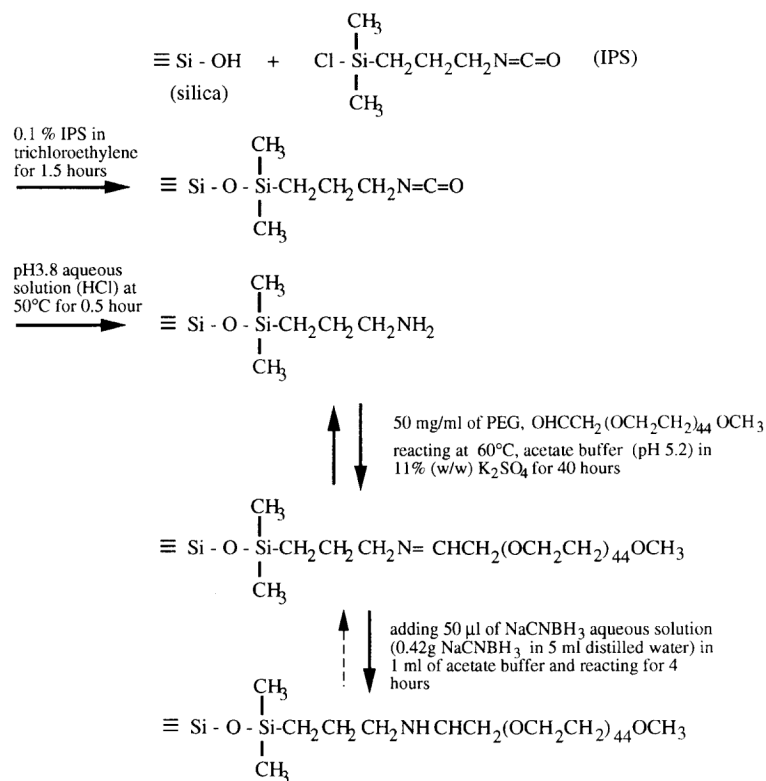
38. Lu DR, Park K. J Colloid Interface Sci. 1991; 144:271.

$$\equiv Si - OH \quad + \quad Cl - \underset{\underset{CH_3}{|}}{\overset{\overset{CH_3}{|}}{Si}} - CH_2CH_2CH_2N{=}C{=}O \quad \text{(IPS)}$$
(silica)

0.1 % IPS in
trichloroethylene
for 1.5 hours
$\longrightarrow$

$$\equiv Si - O - \underset{\underset{CH_3}{|}}{\overset{\overset{CH_3}{|}}{Si}} - CH_2CH_2CH_2N{=}C{=}O$$

pH3.8 aqueous
solution (HCl) at
50°C for 0.5 hour
$\longrightarrow$

$$\equiv Si - O - \underset{\underset{CH_3}{|}}{\overset{\overset{CH_3}{|}}{Si}} - CH_2CH_2CH_2NH_2$$

50 mg/ml of PEG, $OHCCH_2(OCH_2CH_2)_{44}OCH_3$
reacting at 60°C, acetate buffer (pH 5.2) in
11% (w/w) K_2SO_4 for 40 hours

$$\equiv Si - O - \underset{\underset{CH_3}{|}}{\overset{\overset{CH_3}{|}}{Si}} - CH_2CH_2CH_2N{=}CHCH_2(OCH_2CH_2)_{44}OCH_3$$

adding 50 µl of $NaCNBH_3$ aqueous solution
(0.42g $NaCNBH_3$ in 5 ml distilled water) in
1 ml of acetate buffer and reacting for 4
hours

$$\equiv Si - O - \underset{\underset{CH_3}{|}}{\overset{\overset{CH_3}{|}}{Si}} - CH_2CH_2CH_2NHCHCH_2(OCH_2CH_2)_{44}OCH_3$$

Fig. 1.
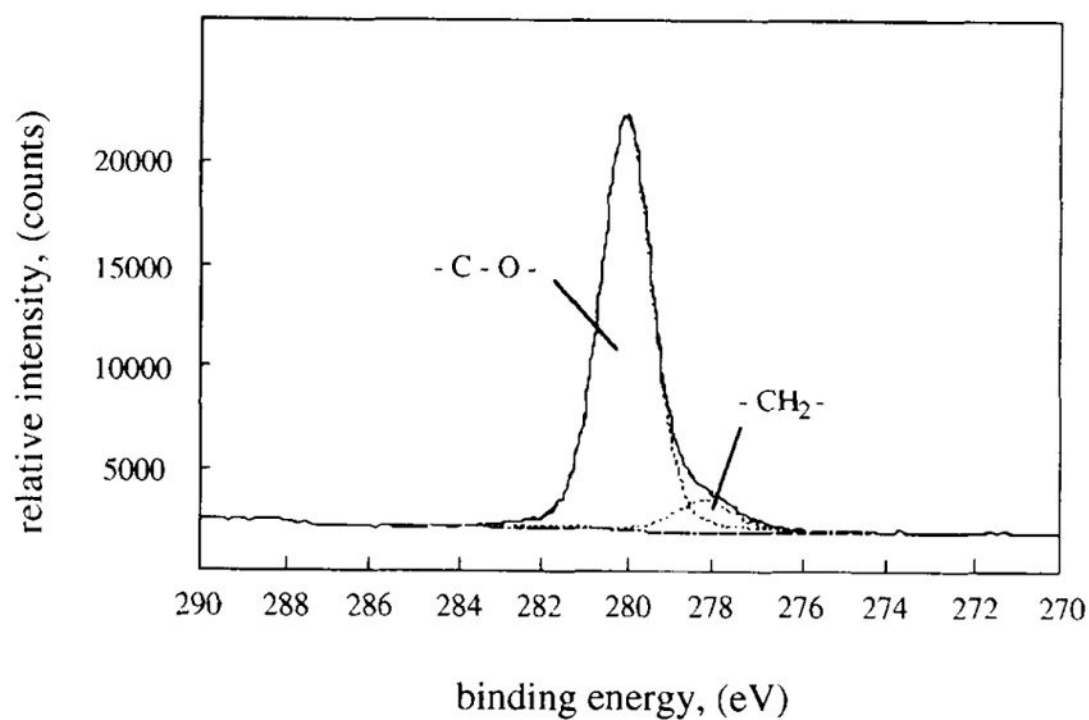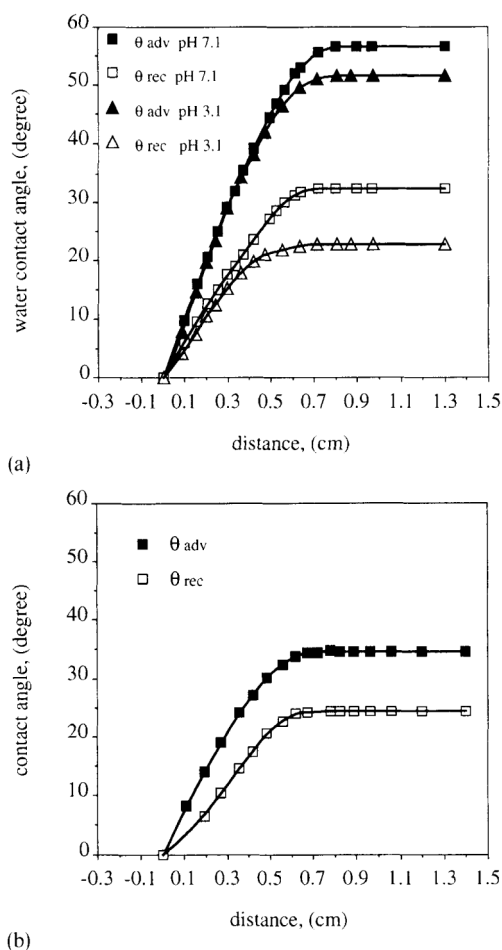Schematics of the preparation of grafted PEG on silica.

Fig. 2.
The XPS spectrum of C1s region of the CH$_3$O–PEG–APDMS silica surface (M_w= 5000 Da).

(a)

(b)

Fig. 3.
(a) The dynamic water contact angles for the APDMS gradient surface shown as a function of gradient position. The silica end of the gradient surface showed $\theta_{adv} = 0°$ and $\theta_{rec} = 0°$. The gradient region and the amine end of the gradient surface showed contact angles dependent on the solution pH. (b) The dynamic water contact angle for the gradient PEG–silica surface shown as a function of gradient position.
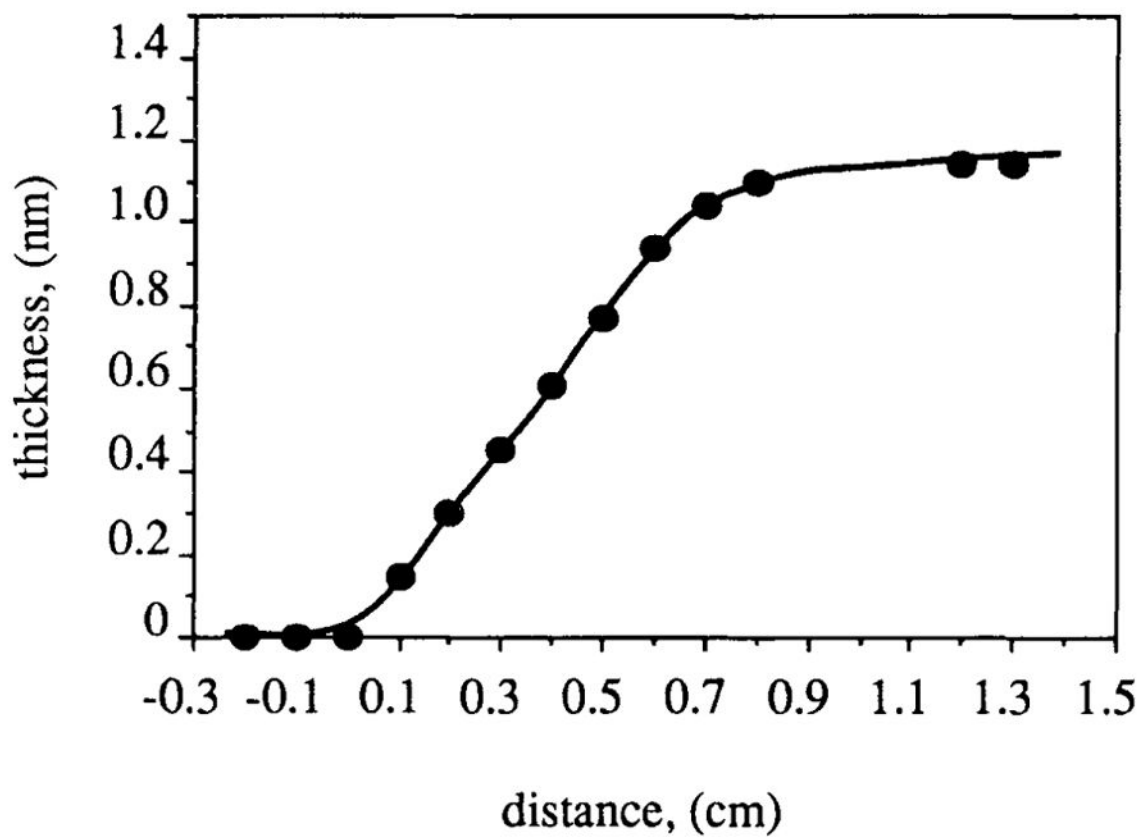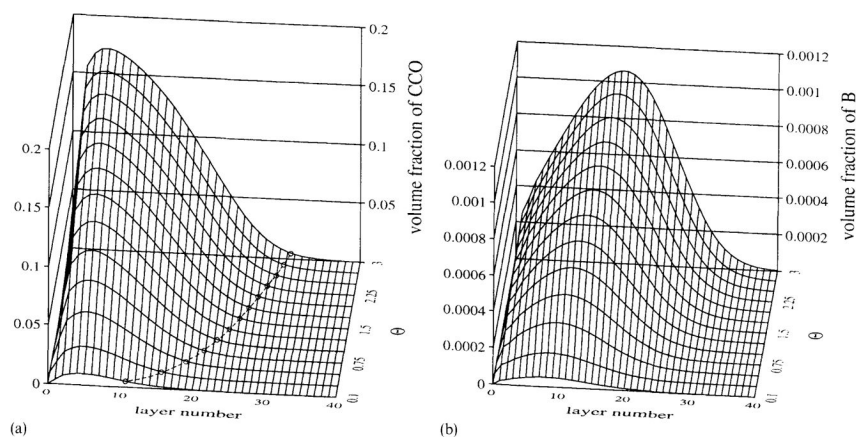
Fig. 4.
The ellipsometric thickness of the CH$_3$O–PEG–APDMS (M_w = 2000Da) layer on an Si/SiO$_2$ surface in air, shown as a function of gradient position.

(a) (b)

Fig. 5.
(a) The volume fraction of CCO segments (simulating PEGs–CH_2CH_2O–) within 40 layers of the solid/water interface shown as a function of the PEG surface density expressed as the number of equivalent monolayers, Θ. The thickness of each layer is 0.1 nm. The broken line indicates the layer in which the volume fraction of PEG segment is below 0.005. (b) The volume fraction of B (simulating the terminal –OCH_3 group) within 40 layers of the solid/water interface shown as a function of the PEG surface density expressed as the number of equivalent monolayers, Θ.
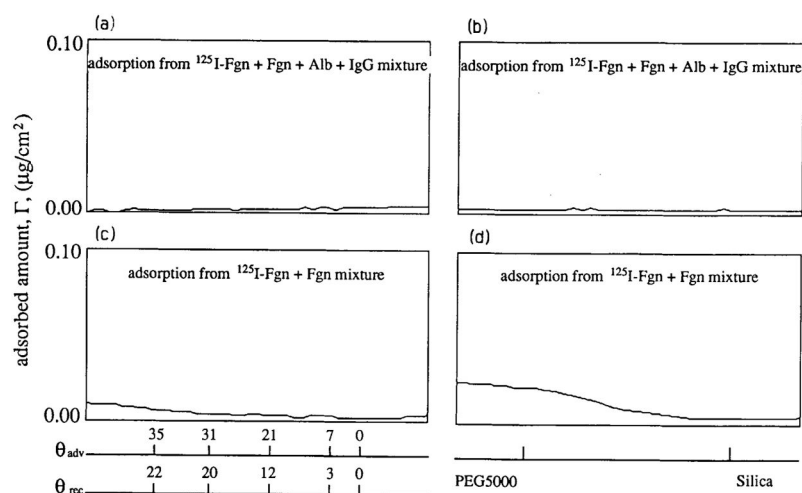
Fig. 6.
Quantified autoradiographic profiles of adsorbed ^{125}I-labeled fibrinogen on the gradient PEG–silica surface shown as a function of the gradient position. In the case of PEG2000, the advancing and receding contact angles are indicated. (a) Fgn adsorption from a ^{125}I-labeled Fgn + Fgn + Alb + IgG mixture on the gradient PEG2000–silica surface;(b) Fgn adsorption from a ^{125}I-labeled Fgn + Fgn + Alb + IgG mixture on the gradient PEG5000–silica surface; (c) Fgn adsorption from a ^{125}I-labeled Fgn + Fgn mixture on the gradient PEG2000–silica surface;(d) Fgn adsorption from a ^{125}I-labeled Fgn + Fgn mixture on the gradient PEG5000–silica surface.

Table 1

Flory–Huggins interaction parameters (kT) for the pairs of components used in the GOLIAD calculation of the PEG segment distribution in the CH$_3$O–PEG surface layer in water

Component	S	W	X	C	O	B
S	0.0	0.0	−300	0.5	0.0	0.5
W	0.0	0.0	0.0	2.0	−1.6	2.0
X	−300	0.0	0.0	0.0	0.0	0.0
C	0.5	2.0	0.0	0.0	2.0	0.0
O	0.0	−1.6	0.0	2.0	0.0	2.0
B	0.5	2.0	0.0	0.0	2.0	0.0

See text for the explanation of the symbols.

Table 2

Reaction conditions and –CO–/–CH$_2$– ratio for PEG2000– and PEG5000– silica surfaces as determined from the respective areas of the deconvoluted C1s XPS spectra

Reaction conditions				XPS intensity ratio –CO–/–CH$_2$–
T (°C)	Time (h)	pH	K$_2$SO$_4$ concentration (%)	
60	40	5.2	11	1.1[a]
60	40	5.2	11	8.6[b]
60	40	5.2	11	10.4[c]
60	40	7.2	11	0[b]
60	40	9.2	11	0[b]

[a]PEG2000, the NaCNBH$_3$ reduction step omitted.

[b]PEG2000 with the NaCNBH$_3$ reduction step.

[c]PEG5000 with the NaCNBH$_3$ reduction step.

Table 3

Relative areas of two deconvoluted XPS peaks in the N1s spectra

Sample		pH	Higher binding energy N1s[a] (eV)	Lower binding energy N1s[a] (eV)
(1)	APDMS	2.94	45 (400.5)	55 (398.5)
(2)	APDMS	7.0	35 (400.8)	65 (398.7)
(3)	PEG2000 + APDMS	7.0	28 (400.8)	72 (399.3)

The XPS counts for samples (1) and (2) were 250–275 for 50 scans, and for sample (3) were approximately 250 for 60 scans.

[a]Maximum energies are given in parentheses.

Table 4

Atomic composition of APDMS, PEG2000– and PEG5000–silica surfaces determined by XPS analysis

Sample	Composition (at.%)				
	C	N	Si	O	$-CO-/-CH_2-$
APDMS	12.8 ± 0.4	1.7 ± 0.3	37.2 ± 0.2	48.2 ± 0.5	-
PEG2000	31.5 ± 0.2	0.8 ± 0.1	22.9 ± 0.1	44.8 ± 0.1	8.6 ± 0.2
PEG5000	40.6 ± 0.2	0.6 ± 0.2	16.9 ± 0.4	42.0 ± 0.1	10.4 ± 1.1

An average for two samples is given.